Eur Biophys J (2008) 37:447–454
DOI 10.1007/s00249-007-0236-1

ORIGINAL PAPER

Thickness distribution of actin bundles in vitro

Lior Haviv · Nir Gov · Yaron Ideses · Anne Bernheim-Groswasser

Received: 14 August 2007 / Revised: 21 October 2007 / Accepted: 26 October 2007 / Published online: 15 November 2007

Abstract Bundles of filamentous actin form the primary building blocks of a broad range of cytoskeletal structures, including filopodia, stereocilia and microvilli. In each case, the cell uses specific associated proteins to tailor the dynamics, dimensions and mechanical properties of the bundles to suit a specific cellular function. While the length distribution of actin bundles was extensively studied, almost nothing is known about the thickness distribution. Here, we use high-resolution cryo-TEM to measure the thickness distribution of actin/fascin bundles, in vitro. We find that the thickness distribution has a prominent peak, with an exponential tail, supporting a scenario of an initial fast formation of a disc-like nucleus of short actin filaments, which only later elongates. The bundle thicknesses at steady state are found to follow the distribution of the initial nuclei indicating that no lateral coalescence occurs. Our results show that the distribution of bundles thicknesses can be controlled by monitoring the initial nucleation process. In vivo, this is done by using specific regulatory proteins complexes.

Keywords Actin bundles · Thickness distribution · Non-equilibrium thermodynamics · Cryo-TEM

Electronic supplementary material The online version of this article (doi:10.1007/s00249-007-0236-1) contains supplementary material, which is available to authorized users.

L. Haviv · Y. Ideses · A. Bernheim-Groswasser (✉)
Ben-Gurion University of the Negev,
Beer-Sheva 84105, Israel
e-mail: bernheim@bgu.ac.il

N. Gov
Weizmann Institute of Science,
Rehovot, Israel

Introduction

The cytoskeleton is a 3D protein network of polar elastic filaments constantly remodeling via the action of a large number of actin binding proteins (ABP's) interacting with the cytoskeletal filaments. As a consequence, in vivo, actin filaments (F-actin) rarely exist as isolated single filaments but instead associate into bundles, e.g., in the case of filopodia (Vignjevic et al. 2006; Adams 2004), stereocilia (Rzadzinska et al. 2004) and microvilli (Majstoravich et al. 2004; Morales et al. 2004), or networks, in concert with these ABP's to support various cellular processes such as motility, division, and adhesion (Pollard and Borisy 2003; Scholey et al. 2003; Bershadsky et al. 2006). The specialized subcellular localization of many F-actin crosslinkers suggests that each of these auxiliary proteins may play a unique role in orchestrating the dynamic organization of actin bundles architectures. In each case, the cell uses specific ABP's to tailor the dimensions, dynamics and mechanical properties of the bundles to suit a specific biological function. In that respect, recent in vivo studies demonstrated the occurrence of a delicate coupling between microvili (Gorelik et al. 2003) and stereocilia (Rzadzinska et al. 2004) dimensions (length) with their internal actin turnover rates. While the length distribution of actin bundles was investigated, both experimentally (Rzadzinska et al. 2004; Gorelik et al. 2003; Popp et al. 2006, 2007; Biron et al. 2006) and theoretically (Biron et al. 2006; Gov 2007), no information on the thickness distribution of actin bundles is available. A previous work studied the average thickness of actin bundles at low concentrations of fascin (Stokes and DeRosier 1991). Another work, studied the average thickness of actin bundles in the presence of polycations (Kwon et al. 2006). One of the conclusions of this study was that the actin bundles

form in two stages; a fast initial formation of a seed of defined diameter, which subsequently grows to form the elongated bundles. Recently, it was further found that the cross-linked actin bundles do not anneal through side-by-side aggregation, while they keep coalescing longitudinally (Lai et al. 2007).

Here, we present an in vitro study of the thickness distribution of actin/fascin bundles. Fascin forms bundles that are unipolar, and is the characteristic bundling protein in filopodia (Adams 2004). It was recently shown, both in vivo (Mejillano et al. 2004) and in vitro (Haviv et al. 2006) that filopodia bundles can originate from a preformed branched actin network. In those studies the thickness of the resulting bundles seems to be tightly regulated by the properties of the originating network, and seem to have a tight normal distribution in their thickness, although these observations were limited by the optical resolution.

Materials and methods

Protein purification and labelling

Actin was purified from rabbit skeletal muscle acetone powder (Spudich and Watt 1971). Recombinant fascin (Ono et al. 1997) was expressed in *Escherichia coli* as a glutathione-*S*-transferase (GST) fusion protein. Actin was labeled on Cys374 with Oregon Green® (Invitrogen).

Cryo-TEM actin/fascin experiments

The following concentrations and ratios of reactants were used for the cryo-TEM experiments: actin 5 μM; [fascin]/[G-actin] = $[F]/[A]$ ratios of 0, 1/200, 1/80, 1/20, 1/5, 1/2, 1/1, 3/1, and 6/1. After mixing the individual components, the system was left to polymerize 1 h at room temperature in polymerization buffer (10 mM 4-(2-hydroxyethyl)-1-piperazineethanesulfonic acid (HEPES), pH 7.6; 5.5 mM dithiothreitol (DTT); 0.12 mM 1,4 diazabicyclo[2,2,2] octane (Dabco); 0.1 M KCl; 2 mM $MgCl_2$; and 1.7 mM Mg-ATP).

Specimens for cryo-TEM were prepared in a controlled environment vitrification chamber (CEVS) (Talmon 1999). All solutions were quenched from 25°C and 100% relative humidity. A volume of 3 μl of the solution was carefully deposited on a TEM grid coated with a holey carbon film (lacey carbon, 300 mesh, Ted Pella, Inc.). The grid was blotted with a filter paper (Whatman no. 1), and plunged into liquid ethane at its freezing point. The vitrified samples were stored under liquid nitrogen before transfer to a TEM (Technai 12, FEI) operated at 120 kV using a Gatan cryo-holder for imaging at −180°C in low-dose mode and with a few micrometers underfocus to increase phase contrast. Images were recorded on multiscan CCD cameras (Gatan 794 or Gatan 791) with the Digital-Micrograph software package and analyzed by METAMORPH (Universal Imaging Co.).

Quantification of number of filaments in bundles

Cryo-TEM images were used to quantify the number of filaments in a bundle, N_b. We analyzed a few hundred bundles to obtain the distributions shown in Fig. 2 and electronic supplementary material (Fig. S1). Considering a bundle as a cylinder or a rod, we calculated the number of filaments N_b from the ratio A_b/A_f, where A_b is the cross-section area of the bundle, given by $A_b = \frac{\pi}{4}D_b^2$ (D_b is measured from the bundles' cross section), and A_f is the effective cross-section area of an actin filament within the bundle, $A_f = \frac{\pi}{4}D_f^2$. The effective diameter D_f corresponds to the typical distance between two actin filaments in an actin/fascin bundle (see Fig. 1e). In our calculation D_f was kept constant at 9 nm (Ishikawa et al. 2003). Note that in the EM pictures we do not resolve individual defects in the packing of the filaments inside the bundles, and we therefore assume that the filaments are compactly organized.

Results

In order to resolve with higher precision the thickness distribution of actin bundles, we conducted high-resolution direct imaging cryo-transmission electron microscopy (cryo-TEM) on solutions of actin/fascin bundles without any branched network progenitor. Such a system is simpler to study and analyze, and also has biological relevance since filopodia bundles formation can proceeds without any pre-existing branched network (Steffen et al. 2006). Comparing Fig. 1a–d, we observed a significant effect on bundle formation when adding increasing amount of fascin. Below a certain fascin concentration [fascin]/[G-actin] = $[F]/[A] < 1/200$]) bundles did not form, we observed only individual actin filaments (Fig. 1a). Above $[F]/[A] = 1/80$ bundles start to form (data not shown), but only in negligible amount. Increasing the amount of fascin generated more and more bundles with respect to individual actin filaments. At $[F]/[A] = 1/5$ and above, straight and well ordered 3D compact bundles of diameter D_b formed (Fig. 1b–d). Below this concentration of fascin, the bundles tend to open-up and form 2D sheets (data not shown), most probably due to shearing during cryo-TEM sample preparation. When the Fascin cross linker concentration is too dilute, the connectivity inside the bundle is so low that a

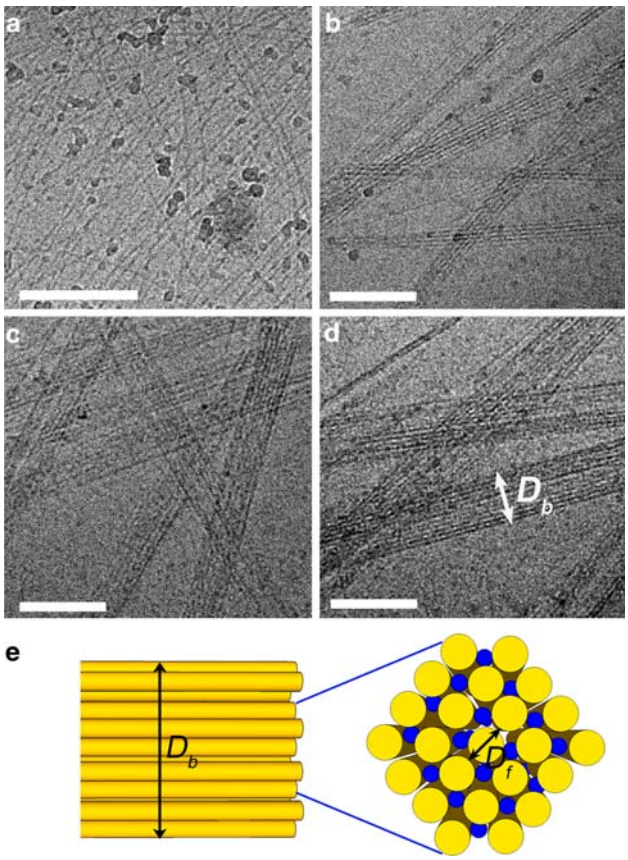

Fig. 1 High-resolution cryo-TEM imaging of actin/fascin bundles. Micrographs were obtained at $[A]$ = 5 μM and variable $[F]/[A]$ ratios of: **a** 1/200, **b** 1/2, **c** 1/1, and **d** 6/1. At very low fascin concentrations (**a**) bundles did not form; only individual actin filaments are seen. Straight compact bundles form above $[F]/[A]$ = 1/5. Their diameter D_b increase with fascin content (**b–d**). *Bars* 0.2 μm. **e** Schematic representation of a bundle. The bundle diameter is D_b (left image, *side view*) and the effective diameter of an actin filament in a bundle is given by D_f (right image, *top view*). The *blue balls* represent fascin cross-linkers and the *yellow circle*, actin filaments. Note that since fascin molecules can attach only at specific sites along the actin filaments (Volkman et al. 2001), the *blue balls* represent attachments of fascin at different highs. In this case the connectivity between actin filaments within the bundle can be rather low

shear force can open the bundle into a flat sheet of side-by-side cross-linked filaments. Note that without the shear the filaments will still form a cylindrical bundle, and similar behavior is observed with other cross-linkers, such as alpha-actinin. Therefore, data analysis was done only on bundles formed above $[F]/[A]$ = 1/5, for which the 3D structure was kept intact. In addition, both fluorescence and cryo-TEM do not show any formation of composite phases or micro-phase separations as sometimes observed in the presence of other ABP's (Tempel et al. 1996; Wagner et al. 2006). We clearly see that the addition of fascin produces bundles of larger diameter. At all fascin concentrations studied, we observe a large polydispersity in the bundles' thicknesses.

The number of filaments per bundle N_b at different fascin concentrations was determined from measurements of bundle diameters D_b on the cryo-TEM images (Fig. 1; see Materials and methods for detailed description of N_b calculation procedure). The mean values of D_b and N_b for the different $[F]/[A]$ ratios, ϕ, studied are given Table S1 (supporting material). We clearly see that the mean size of the bundles increases with fascin concentration.

For all ϕ's, the distribution of N_b, $P(N_b)$, displays the same characteristic behavior (Fig. 2a, b; Fig. S1 of electronic supplementary material): a peak at N_{peak}, followed by an exponential form for large N_b. Long filaments with strong cross-linkers, such that the binding energy per cross-linker is $\sim$10–30 kT and dominates over the entropy, should under ideal conditions condense to form a single bundle of infinite width. This is indeed the minimum energy configuration for a perfectly hexagonal packing of straight, neutral and a-chiral filaments; in this way the loss of binding energy at the rim of the bundle is minimized. Several mechanisms, elastic (Grason and Bruinsma 2007) and electrostatic (Henle and Pincus 2005), have been proposed, that give a finite width distribution for aggregating long filaments. These mechanisms limit the side-by-side aggregation of filaments and result in a finite bundle diameter. In our experiment we have actin filaments that simultaneously nucleate, polymerize, and aggregate in bundles. As shown in Fig. 3 in our system the fascin cross-linker promotes the formation of a stable actin nucleus, composed of short filaments (a few monomers long), which serves as a seed for subsequent actin polymerization. We observe that in this system the actin polymerization is already advanced after about a minute, while without fascin there is a lag-time for nucleation of actin polymerization of order of several minutes (Blanchoin et al. 2001). This dynamic system may therefore be controlled by processes that are not present in an equilibrium aggregation of preformed long filaments, which is the case usually considered theoretically.

We therefore consider the width distribution of the initial disc-like nuclei of the bundles (Fig. 3). Such a system of aggregating elements, in the form of a 2D disc, in thermodynamic equilibrium will either: (1) tend to form an infinitely large aggregate when the attraction forces are dominant, or (2) form a broad distribution of aggregate sizes when the entropy dominates. In the second case the distribution is expected to have an exponential tail, but without a peak. A class of systems that give rise to a peaked distribution of 2D clusters in thermodynamic equilibrium, are those that combine short-range attraction with long-range repulsion (Seul and Andelman 1995), but in our system there is strong screening of such repulsive electrostatic interactions. In addition, since we observe experimentally a prominent peak, we will perform the

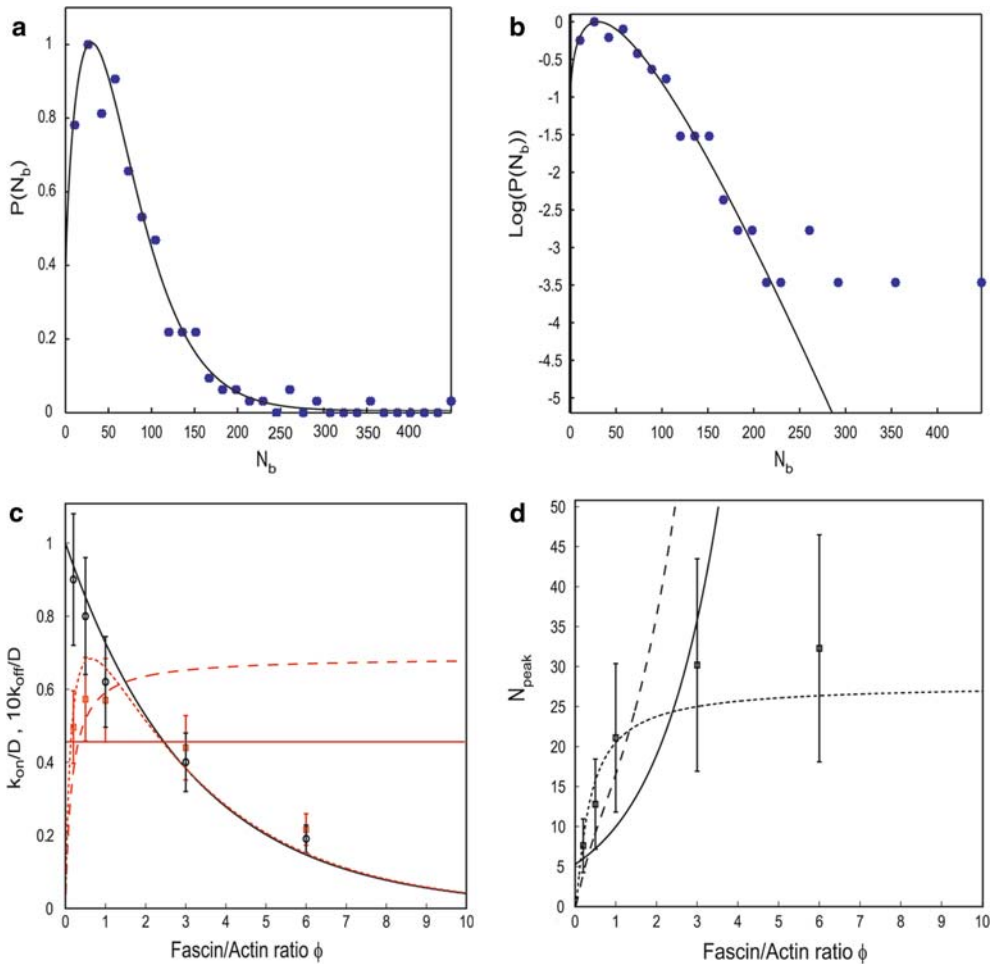

Fig. 2 **a** An example of the measured distribution function $P(N)$ of the actin bundle size N, for a $[F]/[A]$ ratio of 3/1 (*symbols*). The fit using Eq. (1) is given by the *solid line*, and shown as a semi-log plot **b**. Note that for large widths the statistics is noisy, which leads to the observed discrepancy between the fit and the experimental data points **b**. The initial rise, peak and exponential decay are clearly visible. **c** Values of k_{on}/D and k_{off}/D (*black squares* and *red circles*, respectively) that we fitted to the measured distributions, as a function of the $[F]/[A]$ ratio, ϕ. The different fits are described in the text. **d** The values of N_{peak} that we fitted to the measured data (squares). The different fits correspond to those in **c**

analysis using a dynamic model which is not constrained by thermodynamic equilibrium considerations.

We compare the observed distribution functions $P(N_b)$ to the steady-state distribution of a system of aggregating 2D elements (Gov 2006). We find below that the observed distributions indicate that the actin bundle emerges from a flat disc-like nucleus, composed of short actin filaments, possibly containing just several monomers in length, that are cross-linked by fascin. This nucleus forms on a fast time-scale (less than a minute), and then elongates, while the bundle thickness does not change much after the filaments reach their final length (data not shown). This lack of lateral, side-by-side aggregation of bundles, as opposed to longitudinal, was recently observed in vitro (Kwon et al. 2006; Lai et al. 2007).

If side-by-side annealing of long bundles can occur, then the steady-state bundle width distribution that we calculate (Eq. 1 below) will not represent the distribution of the elongated bundles, since the bundles will now be able to aggregate and change their width distribution. The reason that prevents side-by-side annealing is not clear at the moment, and can be due to various physical effects that were recently suggested (Grason and Bruinsma 2007). Since fascin is a very compact and small bundling protein, we expect that it acts as an efficient cross-linker only when there is a very precise alignment and orientation of neighboring filaments. This sensitivity may prevent the efficient side-by-side annealing of long bundles, but allows rapid growth and cross linking when the filaments all elongate together from their initial nucleus.

To test this hypothesis we repeated the experiment with preformed actin filaments, where fascin is added only after the polymerization process has ended. In this system (Fig. 4) we find that the bundles are much less organized,

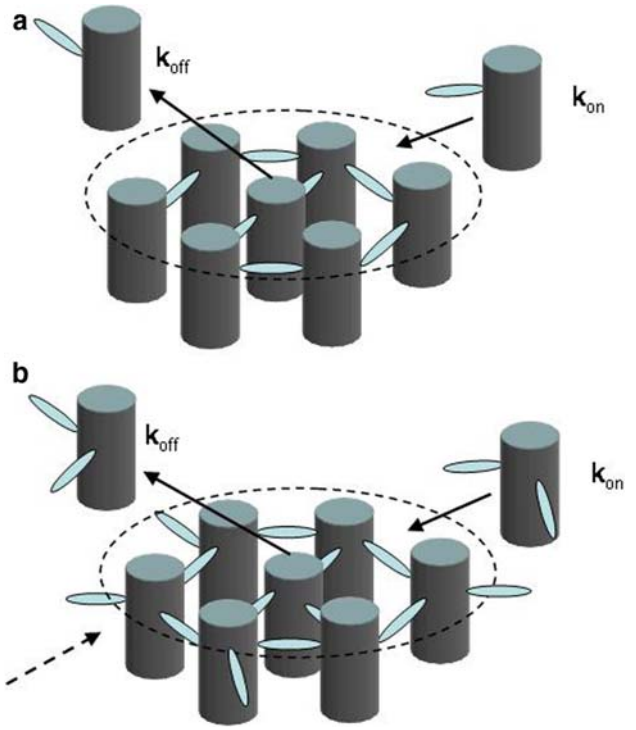

Fig. 3 Dynamics of growth of a disc-like nucleus. **a**, **b** The *cylinders* represent the short actin filaments and the oval objects the fascin cross-linkers. **a** for low $[F]/[A]$ ratios the on-rate is determined by the availability of fascin-attached actin-filaments in the solution. **b** For large $[F]/[A]$ ratios the fascin "coat" on the actin filaments hinders aggregation (*dashed arrow*), which occurs only where fascin is thermally removed (*solid arrows*)

thinner, shorter, and with many defects, compared with the previous case where all the components are mixed in monomeric form (Fig. 4a, c). The bundles in the experiment with the preformed filaments are so disordered and not well defined that we could not extract a meaningful quantitative width distribution. This experiment demonstrates that side-by-side aggregation of preformed actin filaments and bundles is very inefficient, due to physical mechanisms that are still not fully resolved.

In the system studied here the cross-linker, i.e., fascin, attaches specifically to the actin filaments, and is strong enough to overcome the electrostatic repulsion between actin filaments, which are here highly screened by the high salt concentration (see Materials and methods). In this system, equilibrium thermodynamics is expected to give an infinite-sized bundle. The observed finite bundle sizes can be therefore explained as a metastable state due to a non-equilibrium dynamic steady-state. From the fits to the observed distribution (Fig. 2a, b; Fig. S1) we find a plausible dynamic aggregation process, as shown schematically in Fig. 3a. This aggregation process allows new filaments to attach only at the disc rim, while they can be thermally excited to leave the cluster also from its bulk. This kind of dynamic process means that the cluster is packed (Fig. 1e) such that new filaments will attach much more easily at the rim (Fig. 3a) and dominate the growth process. On the other hand, for the dissociation of filaments to occur throughout the bulk of the disc, we conclude that the cross-linking connectivity of the actin filaments inside the disc is therefore low (Fig. 3a). This means that the connectivity of a filament inside the bulk of the cluster is similar to that at the rim, suggesting that short filaments can be thermally excited and leave the cluster just as easily from both regions (Fig. 3a). This low connectivity may follow from the fact that a cross-linker such as fascin (as fimbrin, Volkman et al. 2001) can attach to the actin monomers only at specific sites. Since the filaments in the cluster are short, they can only have a small number of possible attachments per filament, and the connectivity is low. Note that other types of packing defects that were recently considered (Grason and Bruinsma 2007; Upmanyu and Barber 2005) are not relevant during the initial disc formation, where the geometry is very flat and the filaments are very short.

We therefore end up with the boundary-on/bulk-off dynamics (Gov 2006) shown in Fig. 3a, with which we fit the experimental data, for the various $[F]/[A]$ ratios, ϕ (Fig. 2a, b; Fig. S1 in the supporting material). The steady-state size distribution of the disc-like clusters, using this model, is given by (Gov 2006):

$$P(N_b) = R_n e^{2k_{on}\sqrt{N_b}/D} e^{-k_{off}N_b/D}, \quad (1)$$

where k_{on} and k_{off} are the on and off rates, respectively, D represents the noise and fluctuations in this growth process and R_n is a normalization constant. Since we do not know the value of D independently, we give the values of the combined parameters used for the fits in Table 1. The factor f gives the normalized amplitude of the peak of $P(N_b)$ relative to the maximal data point. The value of the peak in the distribution of Eq. (1) is given by: $N_{peak} = (k_{on}/k_{off})^2$. Note that if the filaments have a higher connectivity of cross-linkers in the bulk of the cluster, then they can be excited to leave the cluster only at the rim, and the resulting steady-state distribution is a simple exponential with no peak at a finite cluster size (Gov 2006). The distinct peak that we find in all the distributions, rules out this possible scenario.

In Fig. 2c, d we plot the values of $2k_{on}/D$, k_{off}/D and N_{peak} as a function ϕ. The behavior of N_{peak} for small ϕ's (Fig. 2d) corroborate with the data shown in Fig. 1 of Lieleg et al. (2007). The observed behaviors can be understood from a simple model: The off-rate k_{off} decreases as ϕ increases, since as the number of fascin cross-linkers per short actin filament increases, the energy barrier for dissociation increases, and the off-rate follows from an

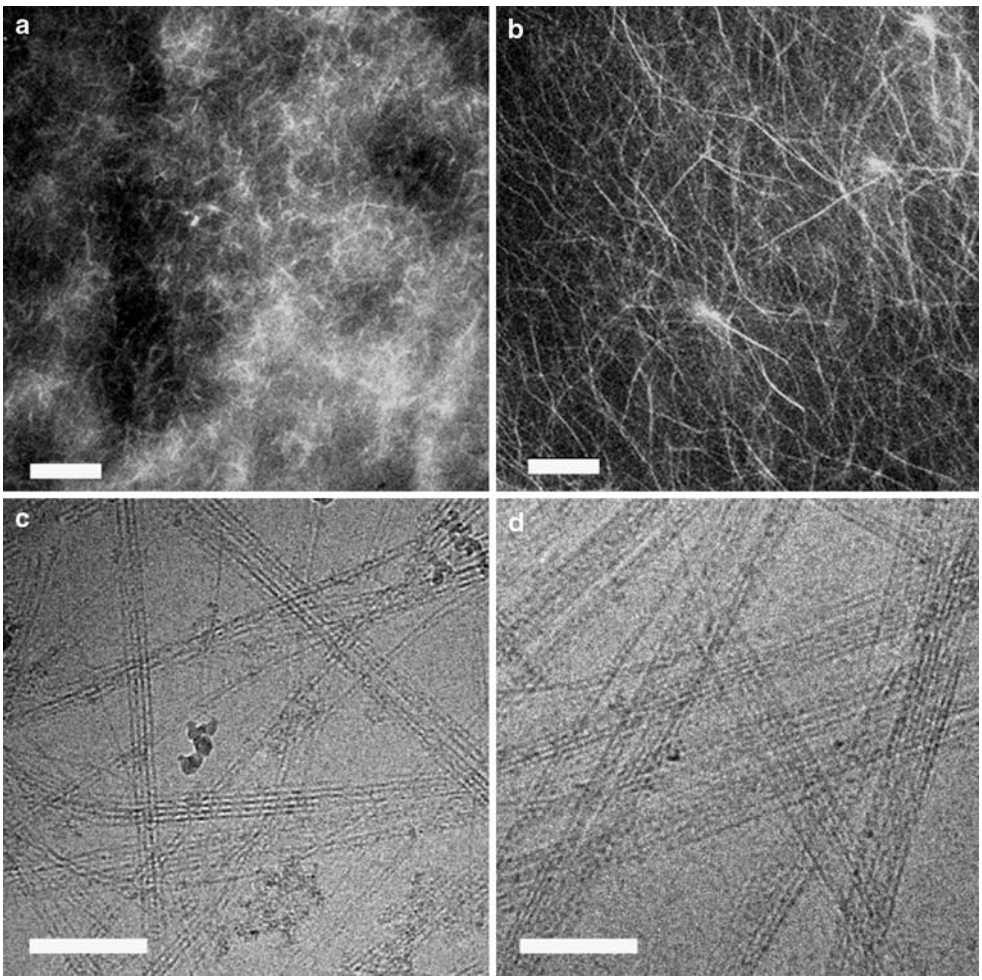

Fig. 4 Assembly routes for actin/fascin bundles formation. Conditions: $[A]/[F] = 1/1$, $(A] = 5$ μM. **a–c** Preformed F-actin filaments were mixed with fascin and left to assemble for 1 h. **b**, **d** Actin/fascin bundles formed by mixing all components in monomeric form. **a** Fluorescence microscopy images of F-actin filaments crosslinked by fascin. The system is composed of short and thin actin filaments/bundles, compared to **b** where the bundles are assembled by a nucleation/growth process. **c** Cryo-TEM image of the same solution as in **a**. The bundles are much less organized, thinner, and with many defects, compared with the case **d** where all the components are mixed in monomeric form. **a**, **b** *Bars* 20 μm. **c**, **d** *Bars* 0.2 μm

Table 1 Parameters used in the fit of the data to the distribution $P(N_b)$ of dynamic disc size, shown in Fig. 2a and b and Fig. S1 in the supporting material

$[F]/[A] = \phi$	$2k_{on}/D$	k_{off}/D	f	N_{peak}
1/5	0.4962	0.09	0.94	7.6
1/2	0.5724	0.08	0.88	12.8
1/1	0.5695	0.062	1.0	21.1
3/1	0.4396	0.04	1.0	30.2
6/1	0.2159	0.019	0.70	32.3

Arhenius thermal excitation process: $k_{off} \propto \exp(-\alpha\phi\varepsilon/k_BT)$, where α is a fit parameter, and ε is the adsorption energy between a fascin molecule and an actin monomer along the filament. When there are more fascin molecules in the solution, more dissociation events have to occur on average during the process of removing a single actin filament. The value of the binding energy of a single fascin–actin bond can be estimated to be: $\varepsilon \approx 10k_BT$ (Borukhov et al. 2005). This exponential behavior is fitted to the observed values of k_{off}/D (solid black line in Fig. 2c, using $\alpha \approx 0.032$), and gives a good agreement. This indicates that the dominant noise in the growth process is independent of ϕ, so that D can be taken to be constant.

The on-rate k_{on} is proportional to the density of actin in the solution n_a, which was kept constant (5 μM) in all experiments. The actin can bind to the cluster rim only when fascin forms a cross-link between two actin filaments, therefore, the relevant concentration is that of actin filaments having an attached fascin molecule (Fig. 3a). This concentration is given by, $n_{af} = n_a p_{fa}$, where p_{fa} is the probability that a short actin filament in the solution is

attached to a fascin cross-linker, given by (Callen 1985): $p_{\mathrm{fa}} = \beta\phi e^{\varepsilon/k_{\mathrm{B}}T}/(1 + \beta\phi e^{\varepsilon/k_{\mathrm{B}}T})$, where $\beta\phi$ is proportional to the fascin volume fraction in the solution. In the limit of no fascin, the on-rate vanishes, while it approaches a constant value at large fascin concentration. In Fig. 2c we plot the fit of both a constant $k_{\mathrm{on}} \propto n_{\mathrm{a}}$ (red solid line) and one including the effect of fascin adsorption, i.e., $k_{\mathrm{on}} \propto n_{\mathrm{af}}$ (red dashed line), which give a reasonable agreement for small ϕ's (using $\beta \approx 2.75 \times 10^{-4}$).

For larger fascin concentrations we find that the on-rate decreases. This effect can arise from the fact that in the limit of large fascin concentrations the fascin molecules cover all the possible attachment points along the short actin filaments in the disc and therefore block their association at the cluster rim (dashed arrow in Fig. 3b). A new filament can bind on to the cluster rim only where there is a thermal fluctuation that breaks some fascin–actin bonds (solid arrow in Fig. 3b). The on-rate now depends on the breaking of existing bonds, enabling addition of a new filament, the same process that drives the off-rate, so that we get, $k_{\mathrm{on}} \propto n_{\mathrm{af}} k_{\mathrm{off}}$. This is shown by the red dotted line in Fig. 2c, and gives a very good agreement with the data. The resulting peak position is now given by $N_{\mathrm{peak}} = (k_{\mathrm{on}}/k_{\mathrm{off}})^2 \propto n_{\mathrm{af}}^2$, also in good agreement with the data (dotted line Fig. 3d). Note that the errors in the determination of the on/off rates ($\pm 20\%$) are estimated by slightly changing the binning of the data, giving rise to larger errors in the peak position due to the quadratic dependence.

Discussion

Long filaments with strong cross-linkers are expected to form a single bundle of infinite width, under ideal conditions. Several mechanisms have been proposed, that give a finite width distribution for aggregating long filaments. One mechanism is based on elastic energy inside the bundle (Grason and Bruinsma 2007), while another is based on electrostatic interactions (Henle and Pincus 2005). In our experiment we have actin filaments that simultaneously nucleate, polymerize, and aggregate in bundles. This dynamic system may therefore be controlled by processes that are not present in an equilibrium aggregation of preformed long filaments, which is the case usually considered theoretically.

In this work we present quantitative information of the thickness distribution of actin/fascin bundles formed in vitro, and show that it has a prominent peak with a wide exponential tail. We further show that this distribution seems to follow from a dynamic model of the growth of an initial flat disc-like shape seed. The good agreement between the observed distribution and the steady-state solution of this dynamic model indicates that following the formation of the initial disc-like nucleus, the actin filaments elongate, but the overall bundle thickness does not change significantly through side-by-side annealing. This was further confirmed by comparison with a system of preformed actin filaments cross-linked by fascin. The width distribution observed when actin and fascin are added in monomeric form therefore reflects the width distribution of the initial nuclei, which is the main proposal of our paper.

Finally, we find that the dynamic rate constants follow a simple Arhenius behavior of thermal excitation over the binding barrier. We find that the peak position of the distribution saturates in the limit of large fascin concentrations, due to the strengthening of the metastability, i.e., the kinetic barrier, resulting from a fascin "coat" hindering further cluster growth.

It will be interesting in the future to observe the shapes and sizes of the initial nucleus of the actin/fascin bundle, which here we could not temporally resolve. It will also be worthwhile to replace fascin with other types of cross-linking proteins, to see if the dynamics described here is universal. It is also interesting to ask if the process of bundling we describe in vitro has any counterpart inside living cells, where the process is regulated by additional proteins.

To conclude, we found here that the thickness distribution of in vitro actin bundles, formed spontaneously due to the presence of one kind of cross-linking protein (fascin), is very wide (exponential), with a distinct peak. This property can be used by cells to maintain a large distribution of membrane protrusions and actin bundles sizes, as in the case of stereocilia hair cells (Rzadzinska et al. 2004) and microvili (Majstoravich et al. 2004). When needed, this can allow cells through the introduction of additional regulating proteins, to select a tighter size distribution (Morales et al. 2004). Our system closely resembles the situation inside the living cell, since also there the nucleation of actin polymerization and cross-linking into bundles always occur simultaneously. In the cell the initial nucleus is formed by specific proteins (such as formins/VASP), from which the actin filaments polymerize and cross-linked to form a bundle (Faix and Grosse 2006). Our experiments show that such a mechanism may allow cells to form well-ordered and compact actin bundles, at a specific location.

Acknowledgments We would like to thank Samuel Safran for many useful discussions. A.B.G wishes to thank the Joseph and May Winston Foundation Career Development Chair in Chemical Engineering, the Israel Cancer Association (grant No. 20070020B) and the Israel Science Foundation (grant No. 551/04). N.G. wishes to thank the Alvin and Gertrude Levine Career Development Chair and the Israel Science Foundation (grant No. 337/05), for their support.

References

Adams JC (2004) Roles of fascin in cell adhesion and motility. Curr Opin Cell Biol 16:590–596

Bershadsky A, Kozlov M, Geiger B (2006) Adhesion-mediated mechanosensitivity: a time to experiment, and a time to theorize. Curr Opin Cell Biol 18:472–481

Biron D, Moses E, Borukhov I, Safran SA (2006) Inter-filament attractions narrow the length distribution of actin filaments. Europhys Lett 73:464–470

Blanchoin L, Amann KJ, Higgs HN, Marchand JP, Kaiser DA Pollard TD (2001) Direct observation of dendritic actin filament networks nucleated by Arp2/3 complex and WASP/Scar proteins. Nature 404:1007–1011

Borukhov I, Bruinsma RF, Gelbart WM, Liu AJ (2005) Structural polymorphism of the cytoskeleton: a model of linker-assisted filament aggregation. Proc Natl Acad Sci USA 102:3673–3678

Callen HB (1985) Thermodynamics and an introduction to Thermostatistics, 2nd edn. Wiley, New York

Faix J, Grosse R (2006) Staying in the shape with formins. Dev Cell 10:693–706

Gorelik J, Shevchuk AI, Frolenkov GI, Diakonov IA, Lab MJ, Kros CJ, Richardson GP, Vodyanoy I, Edwards CR, Klenerman D et al (2003) Dynamic assembly of surface structures in living cells. Proc Natl Acad Sci USA 100:5819–5822

Gov NS (2006) Modeling the size distribution of focal adhesions. Biophys J 91:2844–2847

Gov NS (2007) Theory of the length distribution of tread-milling actin filaments inside bundles. Europhys Lett 77:68005–68011

Grason GM, Bruinsma RF (2007) Chirality and equilibrium biopolymer bundles. Phys Rev Lett 99:098101

Haviv L, Brill-Karniely Y, Mahaffy R, Backouche F, Ben-Shaul A, Pollard TD, Bernheim-Groswasser A (2006) Reconstitution of the transition from lamellipodium to filopodium in a membrane-free system. Proc Natl Acad Sci USA 103:4906–4911

Henle ML, Pincus PA (2005) Equilibrium bundle size of rodlike polyelectrolytes with counterion-induced attractive interactions. Phys Rev E 71:060801R

Ishikawa R, Sakamoto T, Ando T, Higashi-Fujime S, Kohama K (2003) Polarized actin bundles formed by human fascin-1: their sliding and disassembly on myosin II and myosin V in vitro. J Neurochem 87:676–685

Kwon HJ, Tanaka Y, Kakugo A, Shikinaka K, Furukawa H, Osada Y, Gong JP (2006) Anisotropic nucleation growth of actin bundle: a model for determining the well-defined thickness of bundles. Biochemistry 45:10313–10318

Lai GH, Coridan R, Zribi OV, Golestanian R, Wong G (2007) Evolution of growth modes for polyelectrolyte bundles. Phys Rev Lett 98:187802

Lieleg O, Claessens MMAE, Heussinger C, Frey E, Bausch AR (2007) Mechanics of bundled semiflexible polymer networks. Phys Rev Lett 99:088102

Majstoravich S, Zhang J, Nicholson-Dykstra S, Linder S, Friedrich W, Siminovitch KA, Higgs HN (2004) Lymphocyte microvilli are dynamic, actin-dependent structures that do not require Wiskott–Aldrich syndrome protein (WASp) for their morphology. Blood 104:1396–1403

Mejillano MR, Kojima S, Applewhite DA, Gertler FB, Svitkina TM, Borisy GG (2004) Lamellipodial versus filopodial mode of the actin nanomachinery: pivotal role of the filament barbed end. Cell 118:363–373

Morales FC, Takahashi Y, Kreimann EL, Georgescu M-M (2004) Ezrin-radixin-moesin (ERM)-binding phosphoprotein 50 organizes ERM proteins at the apical membrane of polarized epithelia. Proc Natl Acad Sci USA 101:17705–17710

Ono S, Yamakita Y, Yamashiro S, Matsudaira PT, Gnarra JR, Obinata T, Matsumura F (1997) Identification of an actin binding region and a protein kinase C phosphorylation site on human fascin. J Biol Chem 272:2527–2533

Pollard TD, Borisy GG (2003) Cellular motility driven by assembly and disassembly of actin filaments. Cell 112:453–465

Popp D, Yamamoto A, Iwasa M, Maeda Y (2006) Direct visualization of actin nematic network formation and dynamics. Biochem Biophys Res Commun 351:348–353

Popp D, Yamamoto A, Maeda Y (2007) Crowded surfaces change annealing dynamics of actin filaments. J Mol Biol 368:365–374

Rzadzinska AK, Schneider ME, Davies C, Riordan GP, Kachar B (2004) An actin molecular treadmill and myosins maintain stereocilia functional architecture and self-renewal. J Cell Biol 164:887–897

Scholey JM, Brust-Mascher I, Mogilner A (2003) Cell division. Nature 422:746–752

Seul M, Andelman D (1995) Domain shapes and patterns: the phenomenology of modulated phases. Science 267:476–483

Spudich JA, Watt S (1971) The regulation of rabbit skeletal muscle contraction. I. Biochemical studies of the interaction of the tropomyosin–troponin complex with actin and the proteolytic fragments of myosin. J Biol Chem 246:4866–4871

Steffen A, Faix J, Resch GP, Linkner J, Wehland J, Small JV, Rottner K, Stradal TE (2006) Filopodia formation in the absence of functional WAVE- and Arp2/3-complexes. Mol Biol Cell 17:2581–2591

Stokes DL, DeRosier DJ (1991) Growth conditions control the size and order of actin bundles in vitro. Biophys J 59:456–465

Talmon Y(1999) Modern characterization methods of surfactant systems. Marcel Dekker, New York

Tempel M, Isenberg G, Sackmann E (1996) Temperature-induced sol–gel transition and microgel formation in alpha-actinin cross-linked actin networks: a rheological study. Phys Rev E 54:1802–1810

Upmanyu M, Barber JR (2005) Interrupted tubules in filamentous crystals: elastic analysis. Phys Rev B 72:205442

Vignjevic D, Kojima S, Aratyn Y, Danciu O, Svitkina T, Borisy GG (2006) Role of fascin in filopodial protrusion. J Cell Biol 174:863–875

Volkman N, DeRosier D, Matsudaira P, Hanein D (2001) An atomic model of actin filaments cross-linked by fimbrin and its implications for bundle assembly and function. J Cell Biol 153:947–956

Wagner B, Tharmann R, Haase I, Fischer M, Bausch AR (2006) Cytoskeletal polymer networks: the molecular structure of cross-linkers determines macroscopic properties. Proc Natl Acad Sci USA 103:13974–13978